Journal Name

Dynamic Article Links►

Cite this: DOI: 10.1039/c0xx00000x

www.rsc.org/xxxxxx

ARTICLE TYPE

Towards Microstructured Optical Fibre Sensors: Surface Analysis of Silanised Lead Silicate Glass

Herbert T. C. Foo,*[a] Heike Ebendorff-Heidepriem,[a] Christopher J. Sumby,*[a] Tanya M. Monro[a]

Received (in XXX, XXX) XthXXXXXXXXX 20XX, Accepted Xth XXXXXXXXX 20XX

DOI: 10.1039/b000000x

While protocols to surface functionalise silica glass platforms are well-established, the surface coating of other glass types have received limited attention. Here we fully characterise the surface attachment of a fluoroionophore on extruded lead silicate glass slides and demonstrate these slides as a model for investigating the surface chemistry in a microstructured optical fibre (MOF). This model system allows the utilization of multiple, complementary surface-sensitive techniques that cannot be used within the internal surface of the fibre structure. In characterising the fluoroionophore attachment, we observe that the fluorescence intensity from fluorescence imaging, the atomic nitrogen percentage measured by X-ray photoelectron spectroscopy (XPS), the carbonyl bond component (287.5 eV) in the XPS high resolution carbon spectrum, and Principal Component Analysis (PCA) of the time-of-flight secondary ion mass spectrometry (ToF-SIMS) data can be used to provide relative quantification of the concentration of an attached fluoroionophore. We also show the first use of ToF-SIMS imaging and depth profiling of the Pb content within a glass substrate to provide information on the coverage provided by the coating and the relative thickness of an organic coating. Combined, these techniques provide a comprehensive picture of the coated glass surface that facilitates fibre sensor development.

Introduction

Microstructured optical fibre (MOF) based sensors are an emerging class of optical fibre sensor technology that have the potential for low detection limits, flexibility in confined spaces as well as the capacity to measure ultra small volumes (nL to pL) of analyte.[1-9] MOFs can be fabricated from various glass types including silica, tellurite, heavy metal fluoride, bismuth and lead silicate. Non-silica (soft) glasses can be readily fabricated using an extrusion process, which enables the formation of novel optical fibre architectures feasible for sensing applications.[10, 11] Based on the widespread availability of photoinduced electron transfer (PET) fluoroionophores for detection of various cations and anions,[12] we have also used a PET fluoroionophore for sodium sensing in MOFs.[6] Some of us have also demonstrated the possibility of using MOFs in distributed sensing using an exposed core fibre fabricated from soft glass by an extrusion technique.[13] Among many types of soft glass, lead silicates (F2) MOFs have to date been the most widely investigated for chemical and biological sensing.[1] To fabricate a MOF sensor that can be dipped into a sample to enable direct sensing measurements, without requiring the analyte to be mixed with a fluoroionophore, it is necessary to irreversibly – i.e. covalently – immobilise sensor molecules on the glass surface. Methods for covalent attachment are well-established for silica platforms[14] but transfer of these techniques to other materials have not been conclusively validated.

Previously we demonstrated immobilization of fluorescent molecules such as Lumogallion and Quantum-dot labelled antibodies on lead silicate MOFs using organosilane or polyelectrolyte coatings.[7, 15] A key challenge of work in this area is the quantification of the density of the sensor molecules and the quality of the coating on the internal surfaces of the MOFs. These parameters determine the dynamic range and sensitivity of MOF sensors, as well as ensuring reproducible fabrication and/or optimization of surface immobilization procedure, which take place in a constrained volume within the fibre.

Surface characterization within MOFs is challenging. Other glass structures such borosilicate microscopic slides or mechanically polished lead silicate slides have been used as models.[15,7] Although these have a similar glass composition to MOFs they are not fire-polished - smoothed by the surface tension of a low viscosity hot glass surface. Furthermore, the surface glass composition can be modified by treatments such as mechanical polishing.[16] This suggests that better model systems, which are chemically as similar to the internal surface of MOFs, are required for studying surface attachment. In view of this, we have previously studied surface functionalisation on the internal surface of soft glass capillaries as a model system.[17] The internal surface of these capillaries provides a good replica for the internal surface of a MOF since it was prepared by the same fabrication process,[10] however geometric restrictions limit the degree to which the curved surfaces of capillaries can be analyzed.

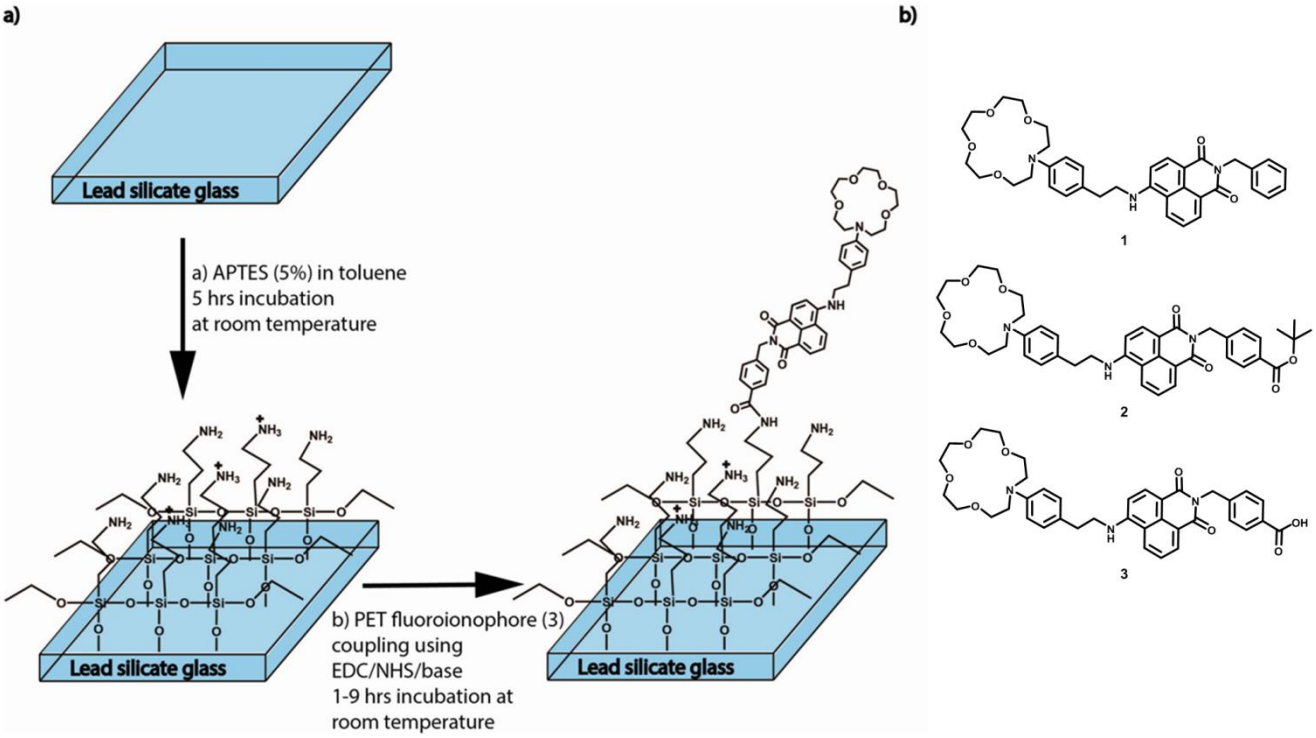

Figure 1. (a) The PET fluoroionophore coating procedure used to generate the coated lead silicate surfaces. (b) The structures of **1**–**3**.

In this paper we demonstrate a powerful approach to characterising the surface attachment chemistry for lead silicate glass that uses a model system based on extruded and hence fire-polished glass slides. These slides are amenable to study by a battery of techniques including scanning fluorescence imaging, X-ray photoelectron spectroscopy (XPS) and Time of Flight secondary ion mass spectroscopy (ToF-SIMS). XPS and ToF-SIMS have been widely used for the quantification and characterization of organic films, biomolecules such as DNA and protein on silicate surfaces.[18-23] Each analysis undertaken provides complementary information for semi-quantitative determination of the surface concentration, relative coating thickness, and coating coverage of an organic molecule, in this case a PET fluoroionophore, on 3-aminopropyltriethoxysilane (APTES) functionalised extruded lead silicate (F2) glass slides (Figure 1). Importantly, the coupling procedure employed is transferable to MOFs. Although there are many combinations of silane reagents and coupling procedures, APTES was chosen in this study because it is one of the most commonly used organosilanes.[16,18] Similarly, the PET fluoroionophore **3** is structurally related to some commercially successful examples of PET fluoroionophores for measuring H^+, Na^+, K^+ and Ca^+.[24] To the best of our knowledge, this is the first comprehensive study of fluoroionophore immobilization on a soft glass surface using fluorescence imaging, XPS and ToF-SIMS.

Experimental

Synthetic Details

The synthesis of **1** has been previously described.[6] The derivatives **2** and **3** were synthesised according to procedures given in the supporting information. All chemicals except tetrahydrofuran (THF) were purchased from Sigma Aldrich and used without further purification. HPLC grade THF was purchased from Scharlau.

Glass preparation

Lead silicate glass slide extrusion. A general description of the extrusion procedure was previously reported.[25] A lead silicate (F2 glass from Schott Co.) glass billet was extruded though a regular extrusion die at high temperature (585°C) to form a flat ribbon with ~1.9 mm cross-section. The ribbon was cut into ~ 10 x 10 mm^2 slide sections using a diamond knife. The bulk composition of F2 glass is 18.7 PbO, 70.7 SiO_2, 5.4 Na_2O, 4.9 K_2O and 0.3 As_2O_3 (mol %).[26]

Slide cleaning. All slides were cleaned first in detergent (~25% Decon90 solution) for 20 minutes in an ultrasonic bath, and then rinsed with reverse osmosis (RO) water thoroughly, followed by another 20 minutes ultrasonic cleaning in HPLC grade methanol. All slides were dried under vacuum overnight.

Surface coating procedures

Ultrasonic cleaning was avoided during all coating procedures since this cleaning step is not transferable to MOF functionalisation. All coated slides were dried under vacuum overnight before further treatment or characterisation.

3-Aminopropyltriethoxysilane (APTES) grafting procedure. Individual cleaned slides were placed in separate vials and incubated in 5 % w/w APTES in anhydrous toluene (< 4 mL) for 5 hours in a desiccator. The slides were washed with toluene (< 4 mL), dried under vacuum for at least 2 hours, before washing with RO water (< 4 mL).

PET fluoroionophore (3) amide coupling. Cleaned APTES coated slides were placed in an individual vial and incubated in 2 mL 9:1 THF: water solution with **3** (0.1 mM, 1 eq.), 1-ethyl-3-(3-dimethylaminopropyl)carbodiimide (EDC) (0.5 mM, 5 eq.), N-hydroxysuccinimide (NHS) (0.5 mM, 5 eq.) and triethylamine (0.15 mM, 1.5 eq.). As the aim of this work was to ascertain methods to characterise these materials, the ratio of EDC and NHS were kept constant at 1:1. Different ratios of EDC and NHS may affect the yield of the surface coupling of fluoroionophore, however, the effect of the ratio is reaction specific and thus the conditions were not optimised here. The incubation was performed at room temperature for 1 – 9 hours. Control experiments were performed at the same time. After incubation, slides were rinsed with THF (< 4 mL × 2), potassium hydrogen phthalate buffer solution (pH 5; < 4 mL × 2) and finally RO water (< 4 mL × 2).

PET fluoroionophore (1, 2 and 3) non-covalent attachment. Cleaned APTES coated slides were placed in an individual vial and incubated in 2 mL 9:1 THF:water solution with **1**, **2**, or **3** (0.1 mM) for 9 hours incubation. After incubation, slides were rinsed with THF (< 4 mL × 2), pH 5 potassium hydrogen phthalate buffer solution (< 4 mL × 2), and finally RO water (< 4 mL × 2).

Surface Analysis

Scanning fluorescence imaging. Surface fluorescence was measured using a Typhoon TM 8600 variable mode imager from Amersham Bioscience. Slides were excited with a 488 nm blue laser and the emission measured through a band pass filter at 520 nm with bandwidth 40 nm. The excitation and emission spectrum of fluoroionophore **3** are given in ESI Figure S4. The measurement method was reported in previous literature.[6] The sensitivity setting used was medium, the resolution for each pixel was 100 μm and the photomultiplier tube (PMT) voltage was 500 V. The average fluorescence intensity per mm^2 of the slides was obtained by measuring 300 data points from three slides per treatment. The measurement error is 1 standard deviation (SD) of 300 data points. To compensate the variation of the instrument laser power between scans performed at different times, an erbium-doped phosphate glass fluorescence standard was scanned at the same time. The composition of the standard was 68.0 P_2O_5, 2.6 MgO, 7.3 CaO, 8.0 ZnO, 7.1 BaO, 0.5 Al_2O_3, 6.4 Yb_2O_3, 0.1 Er_2O_3 (mol %).

X-ray photoelectron spectroscopy (XPS) measurements and data analysis. XPS measurements were performed in an ultra high vacuum apparatus built by SPECS (Berlin, Germany). All the measurements were performed using a non-monochromatic Mg Kα X-ray source and hemispherical Phoibo 100 energy analyser from SPECS. The pressure attained in the analysis chamber is below 5 x 10^{-8} mbar. Charge compensation was performed by electron flood gun SPECS FG20 at 1 eV and 5 μA. The binding energy of Pb 4f7/2 of bare lead silicate glass was calibrated by adventitious carbon (C-H = 284.8 eV).[27] The Pb 4f7/2 in lead silicate glass was 138.6 ± 0.1 eV, which is used as the calibration standard for all the coated glass slides. The Pb 4f7/2 peak was used for calibration because the organic coating material contains an unknown quantity carbonyl groups which will significantly change the carbon peak, whereas Pb from the glass system should have a constant peak position and shape throughout the experiments. The aperture spot diameter was 2 mm and three spots were measurement for each slide. At each sampling spot, a survey spectra with passing energy of 40 eV and a 0.5 eV energy step was collected, followed by high resolution (HR) XP spectra with passing energy of 10 eV and a 0.05 eV energy step. The dwell time of all spectra was 0.1 s. High resolution spectra of C 1s, N 1s, Si 2p, O 2p, Na 1s and Pb 4f were collected.

XPS data fitting was performed using commercial XPS analysis software. A Shirley background was selected to model the background signal. The relative sensitivity factor (RSF) for the X-ray source at 54.7° to the detector for C, N, O, Si, Pb and Na are 0.296, 0.477, 0.711, 0.339, 8.329 and 1.685.[27] These values were used to calculate the atomic percentage of each element from the HR spectra. A convolution of Gaussian (70%) and Lorentzian (30%) peaks were used to fit individual peaks. Peak fitting constrain were introduced in the deconvolution analysis of C and Pb HR spectrum. All components within each HR spectra are assumed to have same full width half maximum (FWHM). In the HR C spectra, three components deriving from the coating were fitted with fixed chemical shift difference relative to CH peak. The chemical shift difference of CH and CN/CO is fixed at 1.5 eV; the difference of chemical shift of CH and C=O is fixed at 3 eV.[28] In Pb HR spectra, two components were fitted with fixed chemical shift at 4.86 eV corresponding to the doublet of 4f7/2 and 4f5/2. The area of the 4f5/2 is fixed at 75 % of the area of 4f7/2.[27]

Time of flight secondary ion mass spectrometry (ToF-SIMS) measurements and analysis. ToF-SIMS experiments were performed using a Physical Electronics Inc. PHI TRIFT V nanoToF instrument (Physical Electronics Inc., Chanhassen, MN, USA) equipped with a pulsed liquid metal ^{79}Au primary ion gun (LMIG), operating at 30 kV energy. Dual charge neutralisation was provided by an electron flood gun and 10eV Ar^+ ions. Experiments were performed under a vacuum of 5x10^{-6}Pa or better. "Bunched" Au_1 instrumental settings were used to optimise mass resolution for spectra; "unbunched" Au_1 instrumental settings were used to optimise spatial resolution for the images. +SIMS spectra were collected from areas of 200 x 200 micron, with an acquisition time of 1 minute. For each sample, six different spots were measured.

Positive ion secondary ion mass spectrometry (+SIMS) images were collected from areas of 100 x 100 micron with an acquisition time of 1 minute. Single-gun depth profile data was also collected using the Au_1 LMIG 'bunched' instrument settings, with an analysis raster of 100 x 100 micron inside a 250 x 250 micron sputter raster. The time of each sputtering cycle is 5 seconds and the acquisition time of the analysis is approximately 15 seconds raw data was collected so that depth profiles of species of interest could be retrospectively produced. For each sample for depth profiling, three measurements were taken from different spots. Sample spectra, images and depth profiles were processed and interrogated using WincadenceN software (Physical Electronics Inc., Chanhassen, MN, USA). For all measurements circular diaphragm (CD) was used to confine the emission angle from the sample.

ToF-SIMS principal component analysis (PCA) was performed using the statistics toolbox in Matlab R2008a. Selected organic fragment ion peaks (see supporting information) were

normalized by the total selected fragment ion peaks before PCA analysis. ToF-SIMS images were exported from WincadenceN software. The distribution of Pb was quantified using Matlab 2008. By subdividing the 100 μm x 100 μm image into 256 separated 16 x 16 pixel sections, the average number of pixels with Pb detected could be counted. Pixel intensity was ignored during the analysis. ToF-SIMS depth profiling data were normalized with the total ion count of that particular spectrum. The final result for each sample is the average normalized ion intensity of all measurement spots on each sample.

Results and discussion

Synthesis and surface attachment

Model PET fluoroionophores **1** and **2** were synthesized by reactions of 4-aminoethyl-phenylaza-15-crown-5 with either*N*-benzyl-4-chloro-1,8-naphthalimide or*t*-butyl-4-chloro-1,8-naphthalimidylmethyl benzoate. The *t*-butyl ester protecting group was removed by hydrolysis using trifluoroacetic acid to afford **3**, which has a carboxyl moiety for covalent attachment to the APTES grafted glass surface, in 8% overall yield. Coupling onto the APTES surface was undertaken under standard peptide coupling conditions using EDC, NHS and triethylamine as the base. Negative controls for the coupling of **3** were obtained by treatment of APTES grafted slides without all or some of the coupling reagents. Without coupling reagents, amide bond formation is not feasible at room temperature.[29]

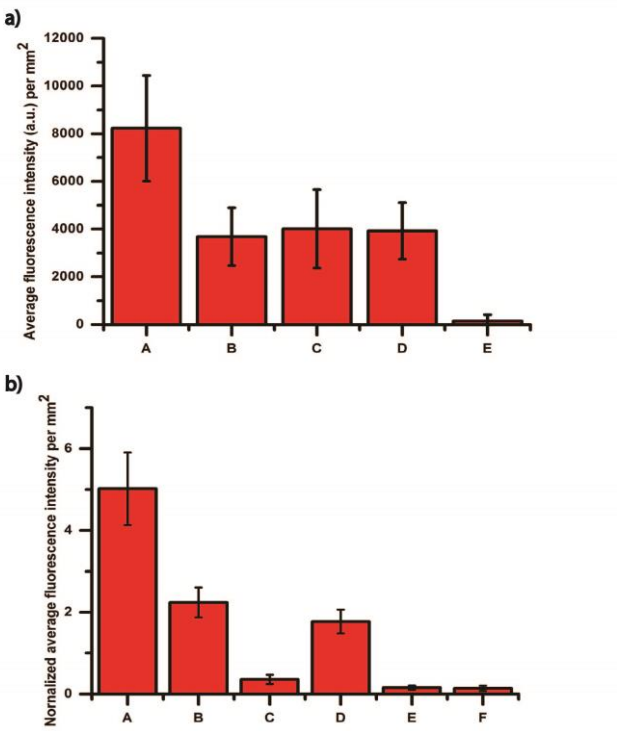

Figure 2. (a) Average fluorescence intensity per mm^2 for slides grafted with APTES and **3** and negative controls. A = **3**/EDC/NHS/base, B = **3** only, C = **3**/NHS/base, D = **3**/base and E = APTES only. (b) Normalized average fluorescence intensity per mm^2 grafted with APTES and **1**, **2** and **3.** A = **3** EDC/NHS/Base, B = **3** only, C = **2** only, D = **1** only, E = APTES only and F = glass.

Surface Analysis

Figure 2(a) shows the average fluorescence intensity per mm^2 of the coated slides. As expected, slides treated with **3** and all coupling reagents show the highest fluorescence intensity compared to the negative controls, with a statistically significant difference. However, all negative controls show significantly higher fluorescence intensity compared to slides with only APTES grafting. This latter observation indicates that **3** also adsorbs non-covalently to APTES coated surfaces after a soft-glass fibre compatible washing procedure, which involves sequential washing with THF, buffer (pH 5) and water. To establish the relationship between surface density of **3** with or without coupling reagents and incubation time, coupling reactions were performed for 1, 5, and 9 hours (ESI Figure S1). No statistically significant difference for samples incubated for 1 – 9 hours was observed, but to ensure the maximum level of coupling was obtained, most analyses were undertaken on samples treated for 9 hours.

To probe whether the non-covalent attachment of **3** on the APTES surface is related to the chemical structure of the fluoroionophore, derivatives **1** and **2** were incubated under the same conditions. Figure 2(b) shows the comparison of fluorescence intensity per mm^2 of all three fluoroionophore derivatives incubated for 9 hours, along with the APTES-grafted and untreated glass slides. Assuming the molar extinction coefficient and quantum yield of all non-covalently attached derivatives on an APTES grafted surface are the same,[30, 31] the quantity of **2** is less than **1** and **3**, while the difference between **1** and **3** is statistically insignificant. These experiments suggest that the fluorophore attachment point has some role in non-covalent binding to the APTES coating. Previous XPS studies on APTES grafted silicon wafers indicated that free primary amine and ammonium groups can co-exist on an APTES coated surface.[28] Thus it is likely that **1** and **3** bind non-covalently to the APTES coated surface through a mixture of charge dipole and electrostatic interactions. It is also possible that the positive ammonium groups are complexed by the crown ether.[32] A difference in solubility of **2** due to the *t*-butyl ester group is consistent with the significantly lower quantities on the APTES surface after washing.

As compounds **1**- **3** are fluoroionophores, they show increased emission intensity upon complexation of sodium or other positive ions of similar size.[6, 33] As a consequence, the interaction of the ionophore with positively charged ammonium ion of the APTES-grafted glass may also change the emission of the fluoroionophore[31] and affect the measurements by scanning fluorescence imaging. Thus, complementary measurements using XPS and ToF-SIMS were performed to corroborate the scanning fluorescence imaging. Importantly, XPS measurements are independent of the molar extinction coefficient and quantum yield and furthermore, the sampling depth of XPS is approximately 10 nm from surface, thus it is ideal for investigating the composition of the chemical coatings and the glass interface.[34]

The Pb 4f7/2 peak was used as the calibration standard throughout these experiments. Since the binding energy of Pb 4f7/2 in this glass composition has not been determined before,

the adventitious carbon shift was used to determine the chemical shift Pb 4f7/2 of the uncoated glass. The Pb 4f7/2 chemical shift of F2 was 138.6 ± 0.1 eV, very close to the literature value for a similar glass composition.[35] APTES-grafted slides coupled to **3**, the negative control without coupling reagents, APTES only coated slides, and bare F2 slides were analysed using XPS. From survey scans, O, C, Si, Pb, Na and N were found in most of the slides. The element quantifications are based on high resolution scans and the summary of the surface elemental analysis can be found in the supplementary information. Previous studies have shown that the reproducibility of grafting for the APTES reagent is highly dependent upon experimental conditions including humidity, temperature, and water content in the solvent and water that is surface-bound on the glass.[36, 37]

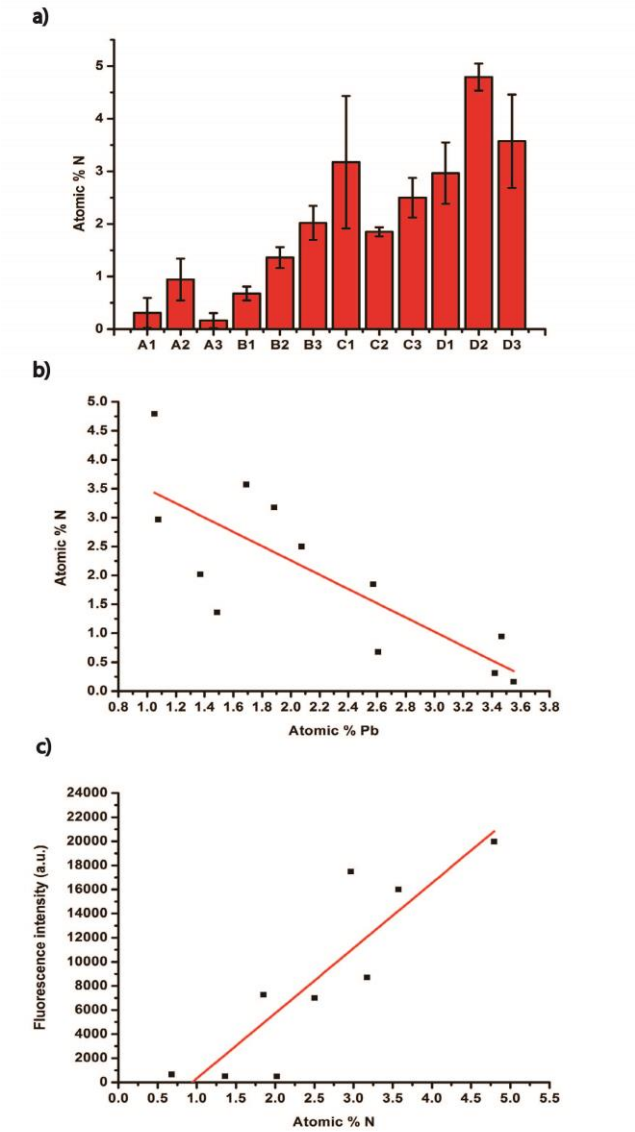

Figure 3. Atomic percentages of (a) nitrogen on bare and coated F2 slides as measured by XPS. A1-A3 = bare glass samples, B1-B3 = APTES grafted glass samples, C1-C3 = **3** and APTES grafted glass without coupling reagents and D1-D3 = **3** and APTES grafted glass with coupling reagents. (b) Nitrogen atomic percentage as a function of lead atomic percentage (R^2 = 0.64). (c) Average fluorescence intensity as a function of nitrogen atomic percentage (R^2 = 0.78).

Figure 3(a) shows the individual atomic percentages of nitrogen in all three samples from each treatment described above. Aside from two individual samples, samples with **3** coupled to the APTES surface were found to have a greater nitrogen content compared to the negative controls and samples with APTES only. Nitrogen is not a component of F2 glass and therefore the nitrogen detected in samples of F2 glass probably reflects surface contamination. The variation of nitrogen content within samples that experienced the same surface treatment may be related to the APTES coating thickness and homogeneity; however, we cannot confirm this hypothesis without ellipsometry and atomic force microscopy that is not possible for these substrates. Figure 3(b) shows the linear correlation between nitrogen and lead content (R^2 = 0.64). The low R^2 is due to the variation of APTES coating which gives a large variation of nitrogen atomic %, while the atomic % of lead among all samples is relatively constant. Despite this, Figure 3b shows a trend of the negative correlation between lead and nitrogen, because the APTES coating is obscuring the lead silicate glass substrate. Figure 3(c) shows that the XPS-measured nitrogen content correlates to the fluorescence intensity (R^2 = 0.78). This correlation arises because the attachment of **3** increases the nitrogen content on the surface, but is partly affected by variation of the APTES coating which also increases the nitrogen content but does not contribute to fluorescence.

To establish a characteristic XPS signal strongly correlated to **3**, we investigated the high resolution (HR) spectrum of carbon in all samples. Using spectral deconvolution, the carbon peak was separated into C-H (284.5 ± 0.1 eV), CN/CO (286 ± 0.1 eV) and C=O (287.5 ± 0.1 eV), see ESI Figures S2(a) - (c). The HR spectra show that samples with **3** coupled to the surface have the highest C=O content. This is reasonable since **3** has three C=O groups, two from the imide and a third from an amide group when **3** is coupled on the surface. Figure 4 shows the correlation (R^2 = 0.88) between fluorescence intensity and the average C=O content on each sample.

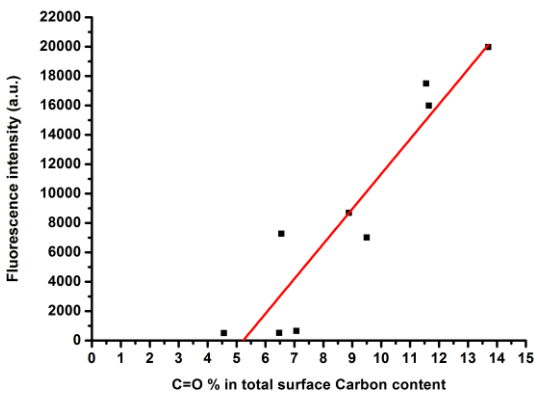

Figure 4. Average fluorescence intensity per mm^2 as a function of the C=O percentage from the deconvolution of the high resolution carbon spectra (R^2 = 0.88).

ToF-SIMS is another surface sensitive technique that can provide non-optical quantification – by mass spectrometry – of the surface density of a chemical. Notably, the sampling depth of the ToF-SIMS is approximately 1-2 nm from the surface, which

means it is a more surface-sensitive technique than XPS. However, mass spectrometry is not usually quantitative so to establish semi-quantitative surface analysis using ToF-SIMS, multivariable statistical analysis based on Principal Component Analysis (PCA) was performed. Figure 5(a) shows the results from the PCA analysis of the +SIMS measurements. PC1 covers 75.1 % and PC2 covers 13.9 % of the covariance of the samples, which gives the total covariance coverage of 89%. Samples are well clustered and separated. Samples with **3**, as well as all necessary coupling reagents, show a negative PC1 projection score, which discriminates samples from all negative controls. A loading plot (supporting information) shows all fragment peaks included in the PCA analysis (also see Table S3a–b for a list of all $C_xH_yN_z$ and $C_xH_yN_zO$ organic fragments which have a significant negative correlation to PC1). These $C_xH_yN_z$ and $C_xH_yN_zO$ organic fragments are related to the structure of **3** and the APTES coating and most of the $C_xH_yN_z$ and $C_xH_yN_zO$ organic fragments are negatively correlated to PC1 and positively correlated to PC2. Samples with **3**/EDC/NHS/base have negative PC1 scores and positive PC2 scores, which matches the pattern for $C_xH_yN_z$ and $C_xH_yN_zO$ organic fragments. Furthermore, PC1 appears correlated to the quantity of **3** attached to the APTES grafted glass surface. Figure 5(b) shows that only samples treated with **3**/EDC/NHS/base have a negative PC1 score, while the rest of the treatments without the full set of coupling reagents and samples with APTES only show positive PC1 scores. The PC1 score of all samples without the full set of coupling reagents show lower PC1 scores compared to samples with APTES only. This difference is statistically significant, and shows the non-covalent attachment of **3** on an APTES grafted surface can be characterised by ToF-SIMS.

Figures 6(a) - 6(d) show ToF-SIMS images for Pb ions in four different samples. The size of each image is 100 µm x 100 µm and the resolution is 256 x 256 pixels; thus, each pixel represents a mass spectrum from a 391 nm x 391 nm sample area. A coloured pixel indicates that Pb was detected with intensity above the ToF-SIMS detection limit. This can be quantified to show the average number of Pb detected pixels in each 6.3 µm x 6.3 µm area of each sample. Thus APTES grafted slides with coupled **3** have the minimum number of Pb detected pixels and, as expected, the Pb ion density is highest in F2 glass. The Pb ion density decreases when APTES was coated on the surface, and shows a further decrease when **3** was coupled on the surface. This result corroborates the negative correlation of N and Pb in the XPS measurements and suggests the Pb ion distribution could be used as a marker to indicate coating coverage on lead silicate glass. Notably, on each slide Pb distribution is relatively random with no significant patchiness observed.

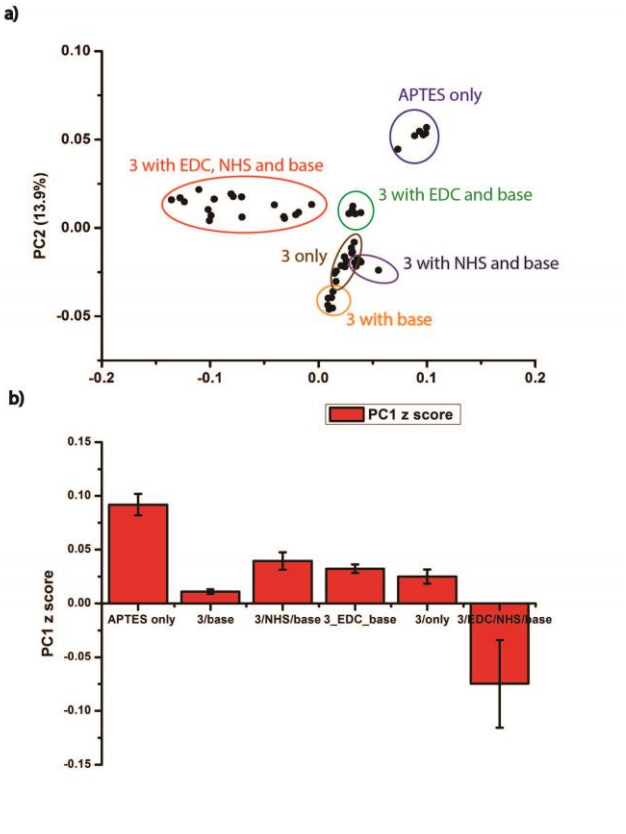

Figure 5. (a) PCA analysis of the ToF-SIMS results. (b) PC1 projection score of all sample types.

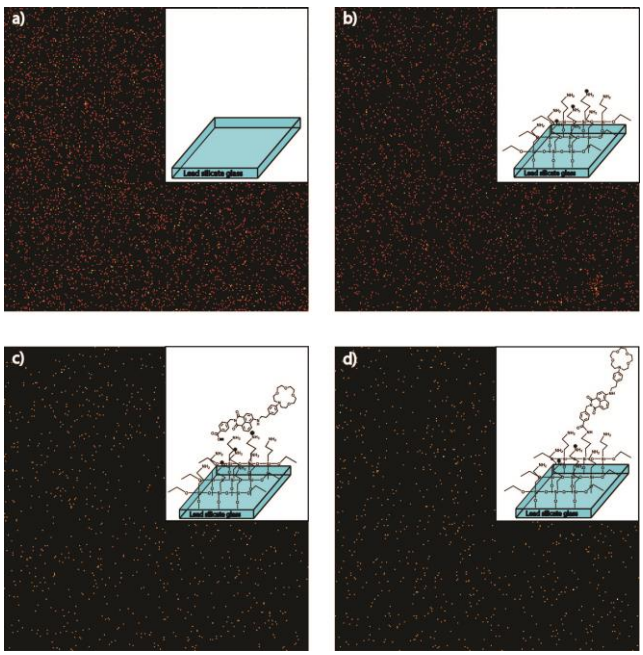

Figure 6. Selected Pb ion images of lead silicate slides with (a) F2 glass, (b) APTES-grafted F2 glass, (c) the negative control and (d) APTES-grafted F2 glass coupled with **3**.

In addition to the quantification of the surface concentration of the coupled fluorophore and the homogeneity of the surface, ToF-SIMS depth profiling can provide information about the relative thickness of a coating. Although in this paper, no calibration was

performed to establish the absolute thickness, as long as the sputtering beam energy is constant, the sputtering time required for the relevant organic fragment peak to reach saturation is proportional to the thickness of the coating. Similar experiments have been previously performed for an organic coating on hard-disk platter, and this approach enables thickness measurements on a thin film (~1 to 2 nm) on a non-reflective surface.[38]

To ensure the depth profiling results are consistent three depth profiles were performed on the same slide to establish the statistical variation within the same sample. The ion intensity was normalized with the total ion intensity from each depth profile. Figure 7(a) shows the depth profile for three identically prepared samples of **3** coupled onto an APTES coated glass surface. It is observed that the normalized peak intensity of Pb increases while CH_4N^+ decreases. Based on the loading plot (see supporting information) of the PCA analysis, it was identified that the CH_4N^+ peak is strongly correlated to the organic coating. These measurements are consistent over the three samples.

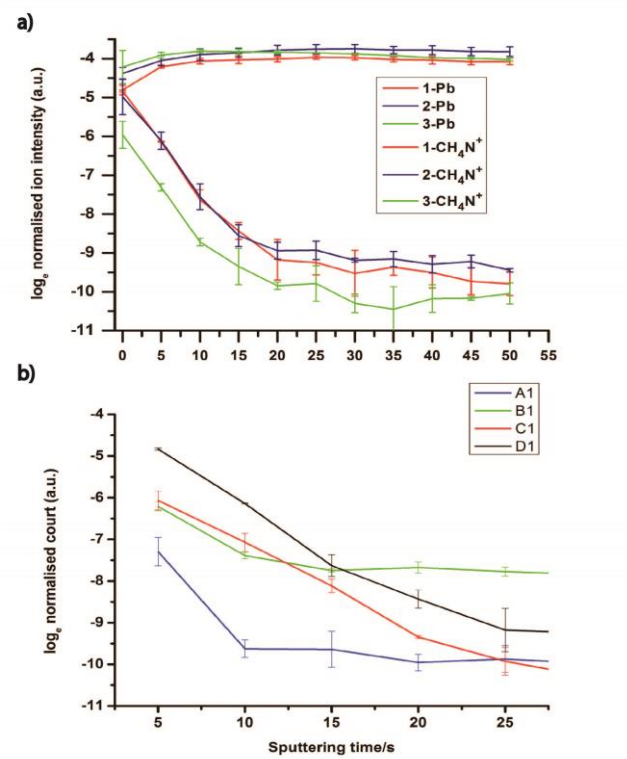

Figure 7. (a) Depth profiles for samples of **3** coupled onto an APTES coated glass surface. (b) CH_4N^+ depth profiling for F2 glass (A1), APTES-grafted F2 glass (B1), the negative control (C1) and APTES-grafted F2 glass coupled with **3** (D1).

Figure 7(b) shows the depth profiling of CH_4N^+ over sputtering time between 5 - 25 seconds on bare F2 slides (A1), APTES only grafted slides (B1), **3** on an APTES grafted surface (C1) and **3** coupled on an APTES grafted surface (D1) as previously studied by XPS. It was observed that the relative intensity of CH_4N^+ for bare F2 slides only fluctuates within statistical error throughout this sputtering time range. The relative intensity of CH_4N^+ for slides with **3** on an APTES grafted surface and **3** coupled on an APTES grafted surface decreased over the period of 5 – 15 seconds, with no statistical difference observed from 15 seconds onwards. In contrast, the relative intensity of CH_4N^+ on APTES only coated samples show no statistical difference from 10 seconds onwards, which indicates the coatings with **3** (negative control and with coupling reagents) are thicker than just the APTES only coating, regardless of the nature of attachment (non-covalent vs. covalent). These results also indicate that the coating thickness of **3** (negative control and with coupling reagents) are similar.

Conclusion

This work has demonstrated the feasibility of performing surface analysis of extruded glass slides as a model system for the internal surfaces of microstructured optical fibres (MOFs) or indeed for any sensing platform based on surface functionalized glass. Surface attachment reactions of **3** were performed using functionalisation conditions feasible for MOFs, meaning that the observations here are transferable to a fibre structure which is traditionally extremely difficult to characterize. Fluorescence imaging identified that attachment of fluoroionophore **3** could occur with or without coupling reagents. This was confirmed by XPS measurements that showed strong correlations of the C=O content in the high resolution carbon spectrum to fluorescence intensity. Through measurement of the C=O content, XPS data was able to identify a difference between covalent and non-covalent fluoroionophore attachment.

PCA of the ToF-SIMS data was able to distinguish the nature of different coatings; in particular, samples with **3** covalently coupled on the glass surface showed a markedly different PC1 projection scores. ToF-SIMS imaging also revealed that the Pb ion distribution could be used as a marker of surface coverage for the coating; the lead distribution is inversely related to the coverage of the glass slide. Furthermore, relative thickness measurements were also performed via depth profiling using ToF-SIMS which identified that slides with model PET sensor attachments, show no difference in thickness regardless of the mode of binding used.

The development of a model extruded glass structure and our validation of methods to characterise these surfaces will enable reaction optimisation of established strategies and the performance of different surface attachment methods to be systematically examined. These include using other silane reagents with different functional groups or polyelectrolytes as the first functional layer, or a single step functionalisation using pre-coupled fluoroionophore and silane reagent that can be directly grafted onto the glass surface. Furthermore, these glass fabrication and characterisation methods are versatile and can be transferred to other glass types capable of being extruded.

Acknowledgements

We acknowledge support from Micromet Pty. Ltd. under the Australian Research Council's Linkage Projects funding scheme (project LP0989605). The surface functionalisation facility within the Adelaide of the Optofab node of the Australian National Fabrication Facility (ANFF) was used. ANFF provides nano and microfabrication facilities for Australian researchers. Dr Gunther Andersson and Ms Natalya Schmerl are thanked for helpful discussions and technical assistance with the XPS measurements.

XPS measurements were performed at the Flinders University in South Australia. We also acknowledge the facilities, and scientific and technical assistance of the Australian Microscopy & Microanalysis Research Facility at the South Australian Regional Facility (SARF), University of South Australia. Dr John Daman is thanked for running the ToF-SIMS measurements and for discussion of the ToF-SIMS data analysis. T.M.M. acknowledges an ARC Federation Fellowship and C.J.S. acknowledges an ARC Future Fellowship (FT0991910).

Notes and references

[a] *Institute of Photonics & Advanced Sensing (IPAS) and School of Chemistry & Physics, The University of Adelaide, South Australia, Australia, SA 5005. CJS: Tel. +61 8 8313 7406. Fax. +61 8 8313 4358. Email: christopher.sumby@adelaide.edu.au; HTCF: Tel. +61 8 8313 2363. Email: tze.foo@adelaide.edu.au*

† Electronic Supplementary Information (ESI) available: All synthetic procedures and NMR, IR and MS characterisation of compound **2** and **3**. Details of additional characterisation experiments, deconvolutions of HR XPS spectra, and the loading plots for the PCA analysis of the TOF-SIMS data. See DOI: 10.1039/b000000x/

1. T. M. Monro, S. Warren-Smith, E. P. Schartner, A. Francois, S. Heng, H. Ebendorff-Heidepriem and S. Afshar, *Opt. Fiber Technol.*, 2010, **16**, 343-356.
2. T. M. Monro, W. Belardi, K. Furusawa, J. C. Baggett, N. G. R. Broderick and D. J. Richardson, *Meas. Sci. Technol.*, 2001, **12**, 854-858.
3. E. P. Schartner, H. Ebendorff-Heidepriem, S. C. Warren-Smith, R. T. White and T. M. Monro, *Sensors*, 2011, **11**, 2961-2971.
4. L. Rindorf, P. E. Hoiby, J. B. Jensen, L. H. Pedersen, O. Bang and O. Geschke, *Anal. Bioanal. Chem.*, 2006, **385**, 1370-1375.
5. V. P. Minkovich, D. Monzon-Hernandez, J. Villatoro and G. Badenes, *Opt. Express*, 2006, **14**, 8413-8418.
6. F. V. Englich, T. C. Foo, A. C. Richardson, H. Ebendorff-Heidepriem, C. J. Sumby and T. M. Monro, *Sensors*, 2011, **11**, 9560-9572.
7. S. C. Warren-Smith, S. Heng, H. Ebendorff-Heidepriem, A. D. Abell and T. M. Monro, *Langmuir*, 2011, **27**, 5680-5685.
8. S. V. Afshar, Y. L. Ruan, S. C. Warren-Smith and T. M. Monro, *Opt. Lett.*, 2008, **33**, 1473-1475.
9. C. Sonnenfeld, S. Sulejmani, T. Geernaert, S. Eve, N. Lammens, G. Luyckx, E. Voet, J. Degrieck, W. Urbanczyk, P. Mergo, M. Becker, H. Bartelt, F. Berghmans and H. Thienpont, *Sensors*, 2011, **11**, 2566-2579.
10. H. Ebendorff-Heidepriem, S. C. Warren-smith, T. M. Monro, *Opt. Express*, 2009, **17**, 2646-2657.
11. H. Ebendorff-Heidepriem, T. M. Monro, *Opt. Express*, 2007, **15**, 15086-15092.
12. A. P. de Silva, T. S. Moody and G. D. Wright, *Analyst*, 2009, **134**, 2385-2393.
13. S. C. Warren-Smith, E. Sinchenko, P. R. Stoddart and T. M. Monro, *IEEE Photonic Tech. L.*, 2010, **22**, 1385-1387.
14. K. Hoffmann, R. Mix, J. F. Friedrich and U. Resch-Genger, in *Reviews in Fluorescence 2008*, ed. C. D. Geddes, Springer, New York, 2010, pp. 139-160.
15. Y. Ruan, T. C. Foo, S. Warren-Smith, P. Hoffmann, R. C. Moore, H. Ebendorff-Heidepriem and T. M. Monro, *Opt. Express*, 2008, **16**, 18514-18523.
16. N. P. Mellott, S. L. Brantley, J. P. Hamilton and C. G. Pantano, *Surf. Interface Anal.*, 2001, **31**, 362-368.
17. T. C. Foo, A. François, H. Ebendorff-Heidepriem, C. J. Sumby and T. M. Monro, in *Australian Conference on Optical Fibre Technology (ACOFT)*, Adelaide, Australia, 2009.
18. J. A. Howarter and J. P. Youngblood, *Langmuir*, 2006, **22**, 11142-11147.
19. H. S. Kim, Y. P. Kim, M. Y. Hong, H. K. Shon, D. W. Moon and T. G. Lee, *Appl. Surf. Sci.*, 2006, **252**, 6801-6804.
20. S. Libertino, F. Giannazzo, V. Aiello, A. Scandurra, F. Sinatra, M. Renis and M. Fichera, *Langmuir*, 2008, **24**, 1965-1972.
21. H. Min, D. W. Moon and T. G. Lee, *Surf. Interface Anal.*, 2011, **43**, 393-396.
22. D. Y. Petrovykh, H. Kimura-Suda, M. J. Tarlov and L. J. Whitman, *Langmuir*, 2004, **20**, 429-440.
23. D. Y. Petrovykh, H. Kimura-Suda, L. J. Whitman and M. J. Tarlov, *J. Am. Chem. Soc.*, 2003, **125**, 5219-5226.
24. J. K. Tusa and H. R. He, *J. Mater. Chem*, 2005, **15**, 2640-2647.
25. H. Ebendorff-Heidepriem and T. M. Monro, *Opt. Mater. Express*, 2012, **2**, 304-320.
26. X. C. Long and S. R. J. Brueck, *Opt. Lett.*, 1999, **24**, 1136-1138.
27. J. F. Moulder, W. F. Stickle, P. E. Sobol and K. D. Bomben, *Handbook of X-ray Photoelectron Spectroscopy*, Physical Electronics, Inc., Minnesota, 1995.
28. R. G. Acres, A. V. Ellis, J. Alvino, C. E. Lenahan, D. A. Khodakov, G. F. Metha and G. G. Andersson, *J. Phys. Chem. C*, 2012, **116**, 6289-6297.
29. E. Valeur and M. Bradley, *Chem. Soc. Rev.*, 2009, **38**, 606-631.
30. A. Hennig, H. Borcherding, C. Jaeger, S. Hatami, C. Würth, K. Hoffmann, T. Thiele, U. Schedler and U. Resch-Genger, *J. Am. Chem. Soc.*, 2012, **134**, 8268-8276.
31. L. L. Wang, A. K. Gaigalas and V. Reipa, *Biotechniques*, 2005, **38**, 127-132.
32. A. Spath and B. Konig, *Beilstein J. Org. Chem.*, 2010, **6**, 32.
33. H. R. He, M. A. Mortellaro, M. J. P. Leiner, S. T. Young, R. J. Fraatz and J. K. Tusa, *Anal. Chem.*, 2003, **75**, 549-555.
34. B. D. Ratner and D. G. Castner, in *Surface Analysis The principal techniques*, eds. J. C. Vickerman and I. S. Gilmore, Wiley, West Sussex, 2009, pp. 47-109.
35. P. W. Wang, L. P. Zhang, L. Lu, D. V. Lemone and D. L. Kinser, *Appl. Surf. Sci.*, 1995, **84**, 75-83.
36. E. Metwalli, D. Haines, O. Becker, S. Conzone and C. G. Pantano, *J. Colloid Interf. Sci.*, 2006, **298**, 825-831.
37. R. M. Pasternack, S. R. Amy and Y. J. Chabal, *Langmuir*, 2008, **24**, 12963-12971.
38. L. Zhu, T. Liew and T. C. Chong, *Appl. Surf. Sci.*, 2002, **189**, 53-58.